Biochimica et Biophysica Acta 1784 (2008) 900–907

Contents lists available at ScienceDirect

Biochimica et Biophysica Acta

journal homepage: www.elsevier.com/locate/bbapap

The kinetic properties producing the perfunctory pH profiles of catalase-peroxidases

Robert L. Moore, Luke J. Powell, Douglas C. Goodwin *

Department of Chemistry and Biochemistry, Auburn University, AL 36849, USA

ARTICLE INFO

Article history:
Received 29 October 2007
Received in revised form 11 March 2008
Accepted 12 March 2008
Available online 21 March 2008

Keywords:
Catalase-peroxidase
KatG
Kinetics
pH-dependence
Substrate-dependent inhibition
Heme

ABSTRACT

Many structure–function relationship studies performed on the catalase-peroxidase enzymes are based on limited kinetic data. To provide a more substantive understanding of catalase-peroxidase function, we undertook a more exhaustive evaluation of catalase-peroxidase catalysis as a function of pH. Kinetic parameters across a broad pH range for the catalase and peroxidase activities of *E. coli* catalase peroxidase (KatG) were obtained, including the separate analysis of the oxidizing and reducing substrates of the peroxidase catalytic cycle. This investigation identified ABTS-dependent inhibition of peroxidase activity, particularly at low pH, unveiling that previously reported pH optima are clearly skewed. We show that turnover and efficiency of peroxidase activity increases with decreasing pH until the protein unfolds. The data also suggest that the catalase pH optimum is more complex than it is often assumed to be. The apparent optimum is in fact the intersection of the optimum for binding (7.00) and the optimum for activity (5.75). We also report the apparent pK_as for binding and catalysis of catalase activity as well as approximate values for certain peroxidatic and catalatic steps.

1. Introduction

Catalase-peroxidases (Kat)[1] are multi-faceted enzymes, having recently been shown to carry out more than the two enzymatic activities they were originally believed to possess, including NADH oxidase, isonicotinic acid hydrazide lyase, and isonicotinoyl-NAD synthase [1]. In addition to their catalytic versatility, there are several medical implications for their structure and function, in particular, their involvement in the activation of the frontline anti-tubercular drug isoniazid [2–4] and their presence as a virulence factor in the periplasmic space of numerous pathogenic bacteria including *Escherichia coli* O157:H7 (food poisoning) [5], *Legionella pneumophila* (Legionnaires' disease) [6,7], and *Yersinia pestis* (bubonic plague) [8,9]. The quickly increasing rate of isoniazid resistance due to KatG mutations [10], in conjunction with the scientific gains that would be made by understanding the mechanism for virulence and multi-functionality, make the study of KatG crucial.

Although the details of the mechanisms of KatG are still under investigation, there are certain aspects of the catalase and peroxidase cycle that are known. Both share a common first step in which the resting enzyme (Por–Fe^{III}) undergoes a two-electron oxidation by a molecule of hydrogen peroxide, creating a ferryl-oxo porphyrin cation radical (Por^+–Fe^{IV}=O) known as compound I and releasing water. Compound I reduction, however, is not similar between the two catalytic pathways. The peroxidase cycle (scheme 1) involves two single electron reduction steps with a reducing compound. The first electron reduces the porphyrin back to a fully covalent state, creating another oxo-ferryl intermediate known as compound II (Por–Fe^{IV}=O) and releasing a molecule of oxidized reducing substrate (commonly a radical). The second electron reduction step restores the enzyme to the resting state releasing water and another molecule of oxidized reducing substrate. In the catalase cycle (scheme 2), compound I is reduced by a second equivalent of hydrogen peroxide, releasing water and molecular oxygen. Interestingly enough, the pH of the environment appears to affect to a greater degree which cycle the enzyme will follow rather than the presence of the appropriate substrates.

The superimposability of the active sites and structural similarity between catalase-peroxidases and monofunctional peroxidases has led to the proposal that KatGs arose from gene duplication and fusion of a predecessor mono-functional peroxidase, followed by more subtle modifications that bestowed catalatic capability on the enzyme [11–13]. This has led to a search for conserved structures of KatGs that are absent in mono-functional peroxidases [14–19]. Many of these searches are based on the reasonable assumption that the active site will have a different configuration based on the pH, considering that the reaction catalyzed by KatG changes with pH. To be able to accurately relate the structure of the enzyme to its function, a complete understanding of its kinetic behavior is necessary. To date, the evaluation of pH-dependency of catalase-peroxidases has involved observing initial rates using single concentrations of substrates, typically at or near saturating conditions [1,20,21]. This method consistently identifies pH optima of 6.5–7.0 for catalase activity and 4.5–5.0 for peroxidase activity.

In efforts to provide a basis for more thoroughly correlating structure and function and its dependence on pH, we performed a full-scale kinetic evaluation to determine the kinetic parameters at pH intervals of 0.25 across the ranges of observed catalytic activity. Through this we discovered the first evidence of ABTS-dependent inhibition of peroxidase

* Corresponding author. Tel.: +1 334 844 6992; fax: +1 334 844 6959.
E-mail address: goodwdc@auburn.edu (D.C. Goodwin).

Abbreviations: Kat, catalase-peroxidases; KatG, *Escherichia coli* catalase peroxidase; ABTS, 2,2′-azino-bis(3-ethylbenzthiazoline-6-sulfonic acid); Por, porphyrin; K_M, Michaelis constant; k_{cat}, turnover number; CD, Circular Dichroism; BpKatG, *Burkholderia pseudomallei* catalase-peroxidase; SynKatG, *Synechocystis* PCC 6803 catalase-peroxidase; MtbKatG, Mycobacterium tuberculosis KatG

1570-9639/$ – see front matter © 2008 Elsevier B.V. All rights reserved.
doi:10.1016/j.bbapap.2008.03.008

$$E + H_2O_2 \rightarrow CpdI + H_2O \qquad k_1$$
$$CpdI + S \rightarrow CpdII + P \qquad k_2$$
$$CpdII + S \rightarrow E + P + H_2O \qquad k_3$$
$$HE + H_2O_2 \rightarrow HCpdI + H_2O \qquad k_4$$
$$HCpdI + S \rightarrow HCpdII + P \qquad k_5$$
$$HCpdII + S \rightarrow HE + P + H_2O \qquad k_6$$
$$E + H^+ \leftrightarrow EH \qquad K_{H1}$$
$$CpdI + H^+ \leftrightarrow HCpdI \qquad K_{H2}$$
$$CpdII + H^+ \leftrightarrow HCpdII \qquad K_{H3}$$

Scheme 1.

activity, most evident at pH values below 4.5. This subsequently revealed that while ABTS acts as the reducing substrate, the optimal pH for peroxidase activity is masked by the inhibition and is not, in fact, 4.5. Also, we present results demonstrating that the lower pH limit for activity is due to an unfolding event. Calculation of the catalase cycle pK_as for the various stages of catalysis for both the interactions between HCpdI and H_2O_2 and the HCpdI–H_2O_2 complex (scheme 2) reveal that the catalase pH optimum of 6.5 is actually the intersection of the optimum for binding (the former) and the optimum for catalysis (the latter).

2. Materials and methods

2.1. Materials

Hydrogen Peroxide (30%), imidazole, hemin, Sephacryl 300 HR, ampicillin, chloramphenicol, citric acid, 2,2′-azino-bis(3-ethylbenzthiazoline-6-sulfonic acid) (ABTS), pyrogallol, and 3,3'-dimethoxybenzidine (*o*-dianisidine) were purchased from Sigma (St. Louis, MO). Isopropyl-β-D-thiogalactopyranoside (IPTG), mono- and di-basic sodium phosphate, acetic acid, hydrochloric acid, and sodium acetate were obtained from Fisher (Pittsburgh, PA). Sodium tartrate was purchased from J.T. Baker Chemical Company (Phillipsburg, NJ). Bugbuster and benzonase were purchased from Novagen (Madison, WI). All *E. coli* strains (BL-21 [DE3] and XL-1 Blue) and Pfu polymerase were obtained from Stratagene (La Jolla, CA). Nickel-nitrilotriacetic acid (Ni-NTA) resin was purchased from Qiagen (Valencia, CA). All buffers and media were prepared using water purified through Millipore Q-PakII system (18.2 MΩ/cm resistivity).

2.2. Expression and purification of wtKatG

Expression and purification of wtKatG was carried out as previously described [22] except that expression cultures were not supplemented with δ-aminolevulinic acid or ferrous ammonium sulfate. Concentration of purified enzyme was estimated according to the method of Gill and von Hippel [23] ($\varepsilon_{280} = 1.44 \times 10^5\ M^{-1}\ cm^{-1}$). A small portion of the purified enzyme had already been incorporated with heme inside the cells. Adding 0.8 heme equivalents directly to the enzyme solution was sufficient to introduce heme to the rest of the enzyme. Reconstituted enzyme solution sat for 72 h to allow unincorporated heme to settle out of solution. The solution was then spun and removed from the precipitated heme. This was to ensure that free heme did not interfere with any spectral or kinetic data. Reconstituted enzyme concentration was then determined using the Soret heme absorption band ($\varepsilon_{408} = 120.7\ mM^{-1}\ cm^{-1}$) [14].

2.3. Peroxidase activity assays

Peroxidase activity was evaluated by monitoring the production of ABTS radical ($\varepsilon_{417} = 34.7\ mM^{-1}\ cm^{-1}$), pyrogallol oxidation ($\varepsilon_{430} = 2.47\ mM^{-1}\ cm^{-1}$), and *o*-dianisidine oxidation ($\varepsilon_{460} = 11.3\ mM^{-1}\ cm^{-1}$) over time; initial ABTS concentration was also determined spectrophotometrically ($\varepsilon_{340} = 3.66 \times 10^4\ M^{-1}\ cm^{-1}$) [24]. All assays were carried out at room temperature on a Shimadzu UV-1601 spectrophotometer (Columbia, MD). Initial velocities were determined across a range of ABTS concentrations while keeping peroxide concentration constant, as well as a range of peroxide concentrations while keeping ABTS concentration constant. Enzyme inhibition (as evidenced by suppressed activity levels) was observed at hydrogen peroxide concentrations greater than 1.0 mM. It was therefore necessary to select a concentration below that of inhibition for performing assays for ABTS-dependent parameter determination; the peroxide concentration, however, was still slightly higher than twice its observed Michaelis constant. For the substrates pyrogallol and *o*-dianisidine, initial velocities were determined across a range of reducing substrate concentrations at a 0.4 mM H_2O_2. The initial velocities (excluding those determined under inhibiting substrate conditions) were fit to the Michaelis equation using a non-linear regression analysis to determine apparent kinetic parameters. Peroxidase assays with ABTS were initially carried out in 50 mM acetate buffer, pH 3.50 to 6.00 in 0.25 pH increments. Recognizing that acetate has little buffering capacity at the extremes of this range, assays were also carried out in 50 mM tartate buffer, pH 3.50 and 3.75 and 100 mM phosphate buffer, pH 6.00. The data obtained using these buffers were the same as the data from assays performed in the acetate buffer. Peroxidase assays with pyrogallol and *o*-dianisidne were carried out in 50 mM acetate buffer, pH 4.00 to 6.00 in 0.5 pH increments.

2.4. Catalase activity assays

Catalase activity was evaluated by monitoring the decrease in H_2O_2 concentration over time at 240 nm ($39.4\ M^{-1}\ cm^{-1}$) [25]. All assays were carried out at room temperature on a Shimadzu UV-1601 spectrophotometer (Columbia, MD). Initial velocities were fit to the Michaelis equation using a non-linear regression analysis to determine kinetic parameters. Accurate determination of catalase activity became increasingly difficult at pH>7 due to the small Michaelis constant for hydrogen peroxide. Measurements carried out below the calculated K_M from preliminary data had initial absorbance below 0.1, and complete consumption of peroxide occurred within 30 s of initiation. To slow the reaction to obtain better initial velocities, enzyme concentration was reduced to 5 nM. Catalase assays were carried out in the following buffers: 50 mM acetate buffer, pH 5.0 to 6.0 in 0.25 pH increments; 100 mM phosphate buffer pH 6.0 to 8.0 in 0.25 pH increments.

2.5. Circular dichroism spectroscopy

All spectra were obtained using 5 μM enzyme in 5 mM citrate buffer (pH 3.10, 3.30, 3.50, 3.60, 3.85) or acetate (pH 3.75, 4.05, 4.20, 4.60, and 4.90) to minimize buffer interference below 200 nm. Acetate had little buffering capacity below pH 3.75, necessitating the overlap of the two buffers. Spectra were recorded at 23 °C in a quartz cell (0.5 mm path length) from 250–195 nm on a Jasco J-810 spectrophotometer (Tokyo, Japan). Baselining and analysis were done using Jasco J-720 software.

2.6. pK_a Determination

Eqs. (1) and (2) (derived in appendix from scheme 1) gave the best fit to the peroxidase kinetic parameters, whereas Eqs. (3) and (4) (derived in appendix from scheme 2) gave the best fit to catalase kinetic parameters.

$$\frac{(k_{cat})_{obs}}{[H_2O_2]} = \left(\frac{k_{cat}}{K_M^{H_2O_2}}\right)_{obs} = \frac{2k_4}{\frac{10^{-pK_{H1}}}{10^{-pH}} + 1} \tag{1}$$

$$\frac{(k_{cat})_{obs}}{[S]} = \left(\frac{k_{cat}}{K_M^{S}}\right)_{obs} = \frac{2k_6}{\frac{10^{-pK_{H3}}}{10^{-pH}} + 1} \tag{2}$$

$$(k_{cat})_{obs} = \frac{k_{cat}}{\frac{10^{-pK_{FO2}}}{10^{-pH}} + 1 + \frac{10^{-pH}}{10^{-pK_{FO1}}}} \tag{3}$$

$$\left(\frac{k_{cat}}{K_M}\right)_{obs} = \frac{\frac{k_{cat}}{K_M}}{\frac{10^{-pK_{F2}}}{10^{-pH}} + 1 + \frac{10^{-pH}}{10^{-pK_{F1}}}} \tag{4}$$

3. Results

3.1. Kinetic parameters for peroxidase activity of KatG

The dramatic and differential effects of pH on the two most prominent activities of catalase-peroxidases have been widely observed

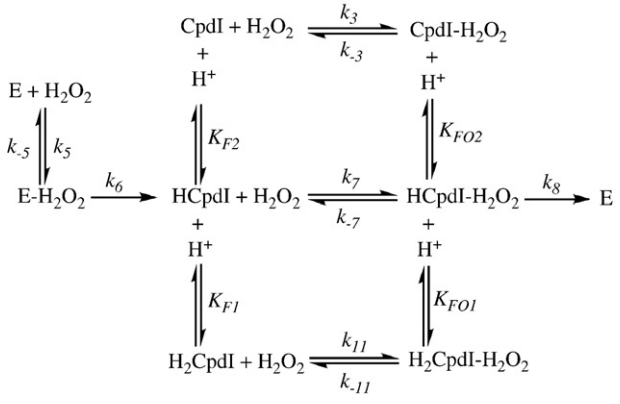

Scheme 2.